TASK QUARTERLY vol. 19, No 3, 2015, pp. 321–351

SIMULATION OF DIFFUSION FLOWS IN TWO-PHASE MULTILAYERED STOCHASTICALLY NONHOMOGENEOUS BODIES WITH NON-UNIFORM DISTRIBUTION OF INCLUSIONS

YEVHEN CHAPLYA[1,2], OLHA CHERNUKHA[2]
AND ANASTASIIA DAVYDOK[2]

[1] *Institute of Mechanics and Applied Informatics*
Kazimierz Wielki University in Bydgoszcz
Kopernika 1, 85-064 Bydgoszcz, Poland

[2] *Centre of Mathematical Modelling of Y. S. Pidstryhach Institute*
of Applied Problems of Mechanics and Mathematics
of the National Academy of Sciences of Ukraine
D. Dudayev 15, 79005 Lviv, Ukraine

(received: 7 April 2015; revised: 29 May 2015;
accepted: 30 Juny 2015; published online: 6 July 2015)

Abstract: Admixture diffusion flows are investigated in two-phase randomly nonhomogeneous multilayered strips with non-uniform distributions of inclusions. Cases where the most probable disposition of layered inclusions is located near the body boundary on which the mass source acts in the neighborhood of another boundary and in the middle of the body are considered. The initial-boundary value problem is formulated for the function of random mass flow under conditions of a constant flow on the upper surface and zero concentration of the admixture on the lower surface. Calculation formulae are obtained for the diffusion flow averaged over the ensemble of phase configurations in the particular cases of beta-distribution at zero and nonzero initial concentrations. The dependences of the averaged admixture flows on medium characteristics are established. It is shown that if the admixture diffusion coefficient in inclusions is greater than in the matrix, consolidation of inclusions in the middle of the body leads to an increasing diffusion flow. Simulation of the averaged diffusion flows of the admixture in the multilayered strip is performed for different model variants of a probable disposition of phases in the body and their comparative analysis is carried out.

Keywords: diffusion process, mass flow, random structure, Neumann series, averaging over the ensemble of phase configurations, beta-distribution

1. Introduction

In many cases there is the important problem of estimation of the effect of random inclusions on the admixture diffusion process in different media. In particular, it may be nonhomogeneous geological structures, composite constructions, multilayered filters, porous materials, nanostructures and so on. As a rule, we know the geometrical and physical characteristics of these inclusions as well as the conditions on the internal contact boundaries.

Until now approaches have been sufficiently developed and mathematical models have been created for determination of distributions of the admixture concentration in the semispace and the layer in the assumption of uniform or gamma-distributions of inclusions in the form of sublayers, parallel-oriented cylinders and spheres [1–6]. However, in many cases, an important characteristic of the diffusion process, in addition to the migrating substance concentration, is the diffusion flow. Owing to the investigation of diffusion flows it is possible to determine the parameters of various kinds of membranes and filters, carry out the estimation of their operation and so on [7–10]. In particular, multilayered filters with different porosities of sublayers are used in the existing industrial systems for treatment of drinkable water and polluted sewage. The efficiency of their operation depends substantially on both the porosity and geometrical parameters of individual elements and the material from which they are made. In the engineering practice, as a rule, simulation and computing are used to solve the corresponding nonlinear problems of filtration by numerical methods.

In determining the mass flows of the admixture in multiphase bodies of a randomly nonhomogeneous structure significant difficulties arise during the procedure of averaging over an ensemble of phase configurations because the functions of correlation between the gradient of the stochastic field of the concentration and the random diffusion coefficient are unknown. One way to solve this problem is the approach proposed in the works [11, 12], in which for porous bodies the authors propose to build balance equations for homogenized media before with physical characteristics being the averaged magnitudes that take into account the difference between coefficients of individual phases. In such case, as a rule, they neglect the interaction between phases. In the works [13, 14] the processes of heat transfer and diffusion in one-dimensional periodical stratified structures are studied on the basis of the method of homogenization, where the authors use the micro-macro approach to describe physical processes and impose certain constraints of admissibility of description for the specific heterogeneous material by some equivalent homogeneous medium. In the paper [15] the random flow is determined after the Darcy low, in which the filtration coefficient is a random function of the spatial coordinate. The methods of both small perturbations and smoothing (with the corresponding constraints) have been applied to construct the problem solution. And also they impose the condition of normal distribution of phases, which makes it impossible to determine the averaged mass flow, therefore the authors define the two-point function of covariation only.

The vital different original approach is proposed in the work [16]. The differential equation for the function of mass flow is obtained from the equation for concentration and the kinetic relation between the mass flow and the gradient of concentration (by the Fick low type). Then, we formulate the correspondent initial-boundary value problems directly for the sought function of the diffusion flow. However, within the scope of such approach we have to formulate the boundary conditions so as to avoid certain possible contradictions. Thus, if the diffusion flow value is larger on the upper body boundary than on its lower surface, then, an unlimited amount of the diffusing substance can enter into a limited body. Similarly, while maintaining a much larger flow through the lower boundary of the layer we also come to certain collisions. In this regard, we propose to set the value of the mass flow on one body surface and the values of the admixture concentration on another surface. Further, we have to find the value of mass flow on this boundary too. In this approach, a random structure of the medium is taken into account in the diffusion coefficient of the migrating substance, in which there is the stochastic function of the spatial coordinates. For solving the initial-boundary value problem of such kind we use the approach developed, for example, in [1] for determining the random field of the admixture concentration. Taking this approach we reduce the formulated diffusion problem to the equivalent integro-differential equation with random kernel for the function of diffusion flow. We find the solution of the obtained equation by the method of successive iterations in the form of the Neumann series as such representation of the solution is convenient for performing the procedure of averaging over an phase configuration ensemble. The theorem on absolutely and uniformly convergent Neumann series as well as the theorem on the existence of the solution of corresponding integro-differential equation is formulated and proved. We also average the stochastic mass flow over the ensemble of phase configurations for the cases when the admixture is initially absent in the body or it is given its nonzero constant initial distribution. Calculation formulae for the averaged mass flow are obtained for the multilayered strip with the uniform distribution of phases [17].

This paper is devoted to study stochastic flows of admixture in two-phase randomly nonhomogeneous stratified bodies at different variants of probable non-uniform distributions of inclusions on the basis of the developed approach.

2. Mathematical model of diffusion flows of admixture particles in stratified bodies

2.1. Problem formulation for the mass flow

Consider the process of the admixture substance diffusion in a strip of thickness z_0 that contains n_0 sublayers of the phase $j = 0$ (matrix) and n_1 sublayers of the phase $j = 1$ (inclusions). The coordinates of sublayer locations are unknown. The volume fraction of the basic phase v_0 is much greater than the volume fraction of inclusions v_1. And the diffusion coefficients are constant within the scope of each phase.

In a one-dimensional spatial coordinate case the equation of admixture diffusion formulated for the function of mass flow in a multiphase body is as follows [18]

$$\frac{\partial J(z,t)}{\partial t} = D(z)\frac{\partial^2 J(z,t)}{\partial z^2} \tag{1}$$

Here $J(z,t)$ is the random mass flow; $D(z) = \begin{cases} D_0, & z \in \Omega_0 \\ D_1, & z \in \Omega_1 \end{cases}$ is the stochastic coefficient of admixture diffusion, Ω_j is the domain of the j-th phase $(j = 0; 1)$.

Let the diffusion flow be absent in the body in the initial moment of time. The constant diffusion flow is supported on the body boundary $z = 0$ and the admixture concentration $c(z,t)$ equals zero on the lower surface of the strip $z = z_0$. Namely, the following initial and boundary conditions are given

$$J(z,t)|_{t=0} = 0 \tag{2}$$

$$J(z,t)|_{z=0} = J_* \equiv \text{const}, \quad c(z,t)|_{z=z_0} = 0 \tag{3}$$

Herewith the diffusion flow on the lower boundary is a certain function of time $F(t)$ that is to determine additionally

$$J(z,t)|_{z=z_0} = F(t) \tag{4}$$

We shall find the function $F(t)$ from the corresponding initial-boundary value problem for the migrating substance concentration.

The condition on the flow (2) means that the admixture concentration can be both zero and nonzero constant in the initial moment. Here we consider both cases.

2.2. Equivalent integro-differential equation. Neumann series

Reduce the problem (1)–(4) to the equivalent integro-differential equation. To do this we introduce a random "function of structure" which does not depend on the medium physical characteristics and satisfies the condition of body continuity [1, 19]:

$$\eta_{ij}(z) = \begin{cases} 1, & z \in \Omega_{ij} \\ 0, & z \notin \Omega_{ij} \end{cases}, \quad \sum_{j=0}^{1}\sum_{i=1}^{n_j} \eta_{ij}(z) = 1 \tag{5}$$

where Ω_{ij} is the i-th simply connected domain of the j-th phase, $\Omega_j = \bigcup_{i=1}^{n_j} \Omega_{ij}$.

The diffusion coefficient is represented by the function η_{ij} as follows

$$D(z) = \sum_{i=1}^{n_0} D_0 \eta_{i0}(z) + \sum_{i=1}^{n_1} D_1 \eta_{i1}(z) \tag{6}$$

If we substitute such representation of $D(z)$ into Equation (1), denote the operators

$$L(z,t) \equiv \frac{\partial}{\partial t} - \left(\sum_{i=1}^{n_0} D_0 \eta_{i0}(z) + \sum_{i=1}^{n_1} D_1 \eta_{i1}(z) \right) \frac{\partial^2}{\partial z^2} \quad L_0(z,t) \equiv \frac{\partial}{\partial t} - D_0 \frac{\partial^2}{\partial z^2} \tag{7}$$

then taking into account the condition of body continuity the diffusion equation can be written as

$$L_0(z,t)J(z,t)=L_s(z,t)J(z,t) \tag{8}$$

where $L_s(z,t)\equiv L_s(z)=L_0(z,t)-L(z,t)=(D_1-D_0)\sum_{i=1}^{n_1}\eta_{i1}(z)\partial^2/\partial z^2$.

Consider the nonhomogeneity of the body structure as inner sources. Then, the solution of the initial-boundary value problem (8), (2)–(4) can be presented by the sum of the solution of the homogeneous problem $J_0(z,t)$ and the convolution of the Green function $G(z,z',t,t')$ with the source. Namely,

$$J(z,t)=J_0(z,t)+\int_0^t\int_0^{z_0} G(z,z',t,t')L_s(z')J(z',t')dz'dt' \tag{9}$$

The Green function has the form [16]:

$$G(z,z',t,t')=\frac{\theta(t-t')}{z_0}\sum_{k=1}^{\infty}e^{-D_0y_k^2(t-t')}\left[\cos\big(y_k(z-z')\big)-\cos\big(y_k(z+z')\big)\right] \tag{10}$$

where $\theta(t-t')$ is the unit step Heaviside function, $y_k=k\pi/z_0$.

To find the solution of the homogeneous problem $J_0(z,t)$ we must determine the values of the flow function on the boundary $z=z_0$. For this purpose we solve the initial-boundary value problem for the function of concentration $c(z,t)$ and apply the first Fick law.

At the condition of zero initial concentration $c(z,t)|_{t=0}=0$ we obtain

$$J_0(z,t)=J_*\left(1-\frac{2}{z_0}\sum_{n=1}^{\infty}\frac{1}{\xi_n}e^{-D_0\xi_n^2t}\sin(\xi_nz)\right) \tag{11}$$

in particular, on the boundary $z=z_0$

$$J_0(z,t)|_{z=z_0}\equiv F(t)=J_*\left(1-\frac{2}{z_0}\sum_{n=1}^{\infty}\frac{1}{\xi_n}(-1)^{n+1}e^{-D_0\xi_n^2t}\right) \tag{12}$$

In the case of the given constant nonzero initial distribution of admixture concentration $c(z,t)|_{t=0}=c_*\equiv\text{const}$ we have

$$J_0(z,t)=J_*-\frac{2}{z_0}\sum_{n=1}^{\infty}e^{-D_0\xi_n^2t}\left(\frac{J_*}{\xi_n}+D_0c_*(-1)^n\right)\sin(\xi_nz) \tag{13}$$

and the expression for the flow on the boundary $z=z_0$ is as follows

$$J_0(z,t)|_{z=z_0}\equiv\tilde{F}(t)=J_*-\frac{2}{z_0}\sum_{n=1}^{\infty}(-1)^{n+1}e^{-D_0\xi_n^2t}\left(\frac{J_*}{\xi_n}+D_0c_*(-1)^n\right) \tag{14}$$

Here $\xi_n=\pi(2n-1)/2z_0$.

Remark that there is discordance between initial and boundary conditions. This statement of the problem with a non-zero initial condition for the admixture concentration is not valid for very small times. For a correct physically justified statement of the initial-boundary value problem it is necessary to introduce an additional transient regime.

We obtain the solution of the integro-differential Equation (9) in the form of the Neumann series by the method of successive iterations [20], namely

$$\begin{gathered} J(z,t)=J_0(z,t)+\int_0^t\int_0^{z_0} G(z,z',t,t')L_s(z')J_0(z',t')dz'dt'+ \\ +\int_0^t\int_0^{z_0} G(z,z',t,t')L_s(z')\int_0^{t'}\int_0^{z_0} G(z',z'',t',t'')L_s(z'')J_0(z'',t'')dz''dt''dz'dt'+\ldots+ \\ +\int_0^t\int_0^{z_0} G(z,z',t,t')L_s(z')\left[\int_0^{t'}\int_0^{z_0} G(z',z'',t',t'')L_s(z'')\times\right. \\ \left.\times\int_0^{t''}\int_0^{z_0} G(z'',z''',t'',t''')L_s(z''')J_0(z''',t''')dz'''dt'''dz''dt''\right]dz'dt'+\ldots \end{gathered} \tag{15}$$

The series (15) is absolutely and uniformly convergent, if the diffusion coefficients are bounded [17] $D_0, D_1 \le K < \infty$ and $D_0 \ne 0$. The first term of the series determines the diffusion flow in the homogeneous layer with matrix characteristics. The second term is the sum of flow disturbances arising when we put inclusions with the characteristics different from the matrix parameters in the body. The third summand describes the effects of pair mutual influence of inclusions on the mass flow that arise when we put alternately pairwise inclusions with another physical parameters in a homogeneous body with matrix characteristics, and so on.

3. Diffusion flows of admixture particles in stratified bodies with non-uniform distributions of inclusions

Consider different variants of inclusion dispositions in the body with different partial cases of the probable β-distribution.

In a general case the function of density of β-distribution is of the form [21]

$$f(z)=\begin{cases} \frac{\Gamma(\alpha+\beta)}{\Gamma(\alpha)\Gamma(\beta)}\left(\frac{z}{z_0}\right)^{\alpha-1}\left(1-\frac{z}{z_0}\right)^{\beta-1}, & z\in[0;z_0] \\ 0, & z\notin[0;z_0] \end{cases} \tag{16}$$

where $\Gamma(x)=\int_0^\infty t^{x-1}e^{-t}dt$ is the Gamma function [22], α, β are degrees of freedom of the distribution.

3.1. Diffusion flow in the two-phase strip with the most probable disposition of inclusions near the "bottom" boundary

We obtain one of the partial cases of the β-distribution (16) if we assume that $\alpha \ge 1$, $\beta = 1$. Then, the density of the distribution takes the form [21]

$$f_1(z)=\begin{cases} \alpha\left(\frac{z}{z_0}\right)^{\alpha-1}, & z\in[0;z_0] \\ 0, & z\notin[0;z_0] \end{cases} \tag{17}$$

We have taken into account that $\Gamma(z+1)=z\Gamma(z)$ [22].

This distribution (Figure 1) is in accord with the structure of a stratified body, in which inclusions dispose near the "bottom" body surface and the phase $j=0$ is situated with probability 1 on the boundary $z=0$, but an inclusion is located on the lower boundary $z=z_0$. And the region of the most probable location of inclusions occurs near this surface (Figures 1 and 2).

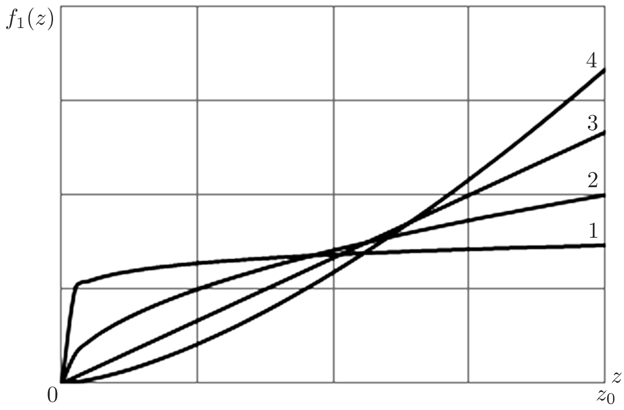

Figure 1. Density of distribution $f_1(z)$ for different degrees of freedom α

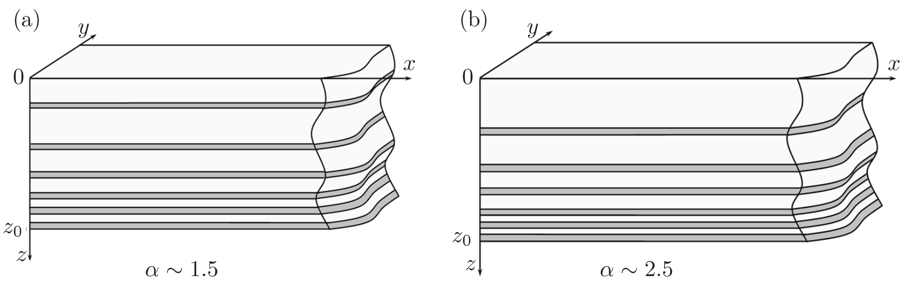

Figure 2. Possible structures of a multilayered strip with $f_1(z)$ distribution of inclusions

Figure 1 shows the dependence of the function of the distribution density $f_1(z)$ on different values of the degree of freedom $\alpha = 1.1$; 1.5; 2; 2.5 (curves 1–4, respectively). Figure 2 illustrates the structures of a multilayered strip corresponding to these distributions. Remark that the probability of inclusion standing near the surface $z=0$ drops with increasing the parameter α as well as sublayers of the phase $j=1$ are compacted in the neighborhood of the surface $z=z_0$ (Figure 2).

For the two-phase multilayered strip with the inner structure of the type shown in Figure 2 the random flow of admixture $J(z,t)$ is described by the diffusion Equation (1). Assume that the constant diffusion flow J_* is supported on the upper body boundary, and the admixture concentration equals zero on the lower body surface, i.e. the boundary conditions (3) are met. Regard, the diffusion flow is absent in the body in the initial moment, then, the condition (2) that corresponds to both zero and nonzero constant initial conditions on the function of concentration is fulfilled.

A solution of the formulated initial-boundary value problem of diffusion in the two-phase multilayered strip with a region of the most probable disposition of inclusions near the lower surface of the strip has been obtained in the form of Neumann integral series (15). Perform the procedure of averaging over the ensemble of phase configurations with the function of distribution of inclusions $f_1(z)$ (17), for that we restrict ourselves by the two first terms of the series (15) and take into account the fact that inclusions have characteristic (average) thickness h_1 as well as the random coordinate characterizing inclusion location is the coordinate of the upper boundary of the sublayer z_{i1} $(i=\overline{1,n_1})$. Then, we find the averaged diffusion flow in the two-phase randomly nonhomogeneous strip by the formula

$$\langle J(z,t)\rangle_{\text{conf}} = J_0(z,t) + (D_1 - D_0)\int_0^t \int_0^{z_0} G(z,z',t,t')\frac{\partial J_0(z',t')}{\partial z^2}\times \\ \times \sum_{i=1}^{n_1} \int_0^{z_0-h_1} \eta_{i1}(z') f_1(z_{i1})dz_{i1}dz'dt' \tag{18}$$

Note that we have used the following relation

$$\sum_{i=1}^{n_1}\langle \eta_{i1}(z')\rangle = \sum_{i=1}^{n_1}\int_{(V)} \eta_{i1}(z') f_1(z_{i1})dz_{i1} \tag{19}$$

Taking into consideration of properties of the function $\eta_{i1}(z')$

$$\eta_{i1}(z') = \begin{cases} 1, & z' \in [z_{i1};\, z_{i1}+h_1] \\ 0, & z' \notin [z_{i1};\, z_{i1}+h_1] \end{cases} = \begin{cases} 1, & z'-z_{i1} \in [0;\, h_1] \\ 0, & z'-z_{i1} \notin [0;\, h_1] \end{cases} = \eta_{i1}(z'-z_{i1}) \tag{20}$$

and performing a change of the variable $z'-z_{i1}=x$ we can write

$$\sum_{i=1}^{n_1}\langle \eta_{i1}(z')\rangle = \sum_{i=1}^{n_1}\int_0^{z_0-h_1} \eta_{i1}(z'-z_{i1}) f_1(z_{i1})dz_{i1} = \sum_{i=1}^{n_1}\int_0^{z'} \eta_{i1}(x) f_1(z'-x)dx \tag{21}$$

Substitute the function of distribution density (17) into (21). Then, we obtain

$$\sum_{i=1}^{n_1}\langle \eta_{i1}(z')\rangle = \alpha(z_0)^{1-\alpha}\sum_{i=1}^{n_1}\int_0^{z'} \eta_{i1}(x)(z'-x)^{\alpha-1}dx \tag{22}$$

The integral in the obtained formula depends on the value of the variable of exterior integration z' in the expression (18). Therefore

(1) if $z' \le h_1$ then

$$\sum_{i=1}^{n_1} \int_0^{z'} \eta_{i1}(x)(z'-x)^{\alpha-1}dx = \sum_{i=1}^{n_1} \int_0^{z'} (z'-x)^{\alpha-1}dx = \frac{n_1(z')^\alpha}{\alpha} \tag{23}$$

(2) if $z' \ge h_1$ then

$$\sum_{i=1}^{n_1} \int_0^{z'} \eta_{i1}(x)(z'-x)^{\alpha-1}dx = \sum_{i=1}^{n_1} \int_0^{h_1} (z'-x)^{\alpha-1}dx = \frac{n_1\big((z')^\alpha - (z'-h_1)^\alpha\big)}{\alpha} \tag{24}$$

With provision for $v_1 = n_1 h_1/z_0$ finally we obtain the expression for the density of distribution $f_1(z)$

$$\sum_{i=1}^{n_1} \langle \eta_{i1}(z') \rangle = \frac{v_1}{h_1 z_0^{\alpha-2}} \begin{cases} z'^\alpha, & z' \le h_1 \\ z'^\alpha - (z'-h_1)^\alpha, & z' \ge h_1 \end{cases} \tag{25}$$

Substituting (25) into the relation (18) we obtain the formula for finding the flow of admixture particles in a two-phase strip with a region of the most probable disposition of inclusions near the lower surface averaged over the ensemble of phase configurations:

$$\begin{aligned} \langle J(z,t) \rangle = J_0(z,t) + \frac{(D_1-D_0)v_1}{z_0^{\alpha-2}h_1} \int_0^t \Bigg[\int_0^{h_1} z'^\alpha G(z,z',t,t') \frac{\partial^2 J_0(z',t')}{\partial z'^2} dz' + \\ + \int_{h_1}^{z_0} (z'^\alpha - (z'-h_1)^\alpha) G(z,z',t,t') \frac{\partial^2 J_0(z',t')}{\partial z'^2} dz' \Bigg] dt' \end{aligned} \tag{26}$$

If we substitute the expressions for both the Green function $G(z,z',t,t')$ (10) and the diffusion flow in the homogeneous body $J_0(z,t)$ (11) into the formula (26), then we obtain the calculation formula for the diffusion flow averaged over the ensemble of phase configurations at the zero initial concentration of admixture in the body

$$\begin{aligned} \frac{\langle J(z,t) \rangle}{J_*} = 1 - \frac{2}{z_0} \sum_{n=1}^{\infty} \frac{1}{\xi_n} e^{-D_0 \xi_n^2 t} \sin(\xi_n z) + \frac{2(D_1-D_0)v_1}{D_0 z_0^\alpha h_1} \times \\ \times \sum_{k=1}^{\infty} \sum_{n=1}^{\infty} \frac{\xi_n}{y_k^2 - \xi_n^2} \left(e^{-D_0 \xi_n^2 t} - e^{-D_0 y_k^2 t} \right) A_{kn}^{(1)} \sin(y_k z) \end{aligned} \tag{27}$$

where $A_{kn}^{(1)} = f(0,x_{kn}^-) - f(0,x_{kn}^+) - f(h_1,x_{kn}^-) + f(h_1,x_{kn}^+)$, $x_{kn}^\pm = y_k \pm \xi_n$, $f(a,p) = \int_a^{z_0} (z-a)^\alpha \cos(pz) dz$.

If a constant nonzero distribution of admixture concentration in the initial moment is imposed, then we substitute the expression (13) for the flow in the homogeneous layer $J_0(z,t)$ into the formula (26). And the calculation formula for the averaged mass flow at nonzero initial concentration takes the form

$$\frac{\langle J(z,t)\rangle}{J_*} = 1 - \frac{2}{z_0}\sum_{n=1}^{\infty} e^{-D_0\xi_n^2 t}\left(\frac{1}{\xi_n} + (-1)^n \frac{D_0 c_*}{J_*}\right)\sin(\xi_n z) +$$
$$+ \frac{2(D_1 - D_0)}{D_0 z_0^{\alpha}}\frac{v_1}{h_1}\sum_{k=1}^{\infty}\sum_{n=1}^{\infty}\frac{\xi_n}{y_k^2 - \xi_n^2}\left(1 + (-1)^n \frac{D_0 c_*}{J_*}\xi_n\right)\left(e^{-D_0\xi_n^2 t} - e^{-D_0 y_k^2 t}\right)\times$$
$$\times\big(f(0, y_k - \xi_n) - f(0, y_k + \xi_n) - f(h_1, y_k - \xi_n) + f(h_1, y_k + \xi_n)\big)\sin(y_k z) \tag{28}$$

Remark that the formulae (27) and (28) contain integral summands for computation of the averaged diffusion flows at zero and nonzero initial concentration and they require methods of numerical integration for numerical analysis. Here we use the method of trapezoids [23].

3.2. Simulation of averaged diffusion flows in the strip with the most probable disposition of inclusions near the "bottom" boundary

On the basis on the formulae (27) and (28) software modules have been designed for computation of the averaged diffusion flows of admixture in the two-phase stratified strip with a region of the most probable disposions of inclusions near the "bottom" boundary of the body. Numerical calculations are performed in the dimensionless variables [24]

$$\varsigma = z/z_0 \quad \tau = D_0 t/z_0^2 \tag{29}$$

We set the following basic parameters of the problem $\tau = 0.1$; $v_1 = 0.2$; $h_1 = 0.01$; $\alpha = 2.5$; $c_*/J_* = 0.1$.

In Figure 3 distributions of the averaged mass flows are illustrated in different dimensionless moments of time $\tau = 0.01$; 0.03; 0.1; 0.5; 1 (curves 1–5). Figure 4 shows distributions of mass flows in the strip for different values of the ratio of diffusion coefficients $D_1/D_0 = 0.01$; 0.5; 2; 5; 10; 15; 20 (curves 1–7).

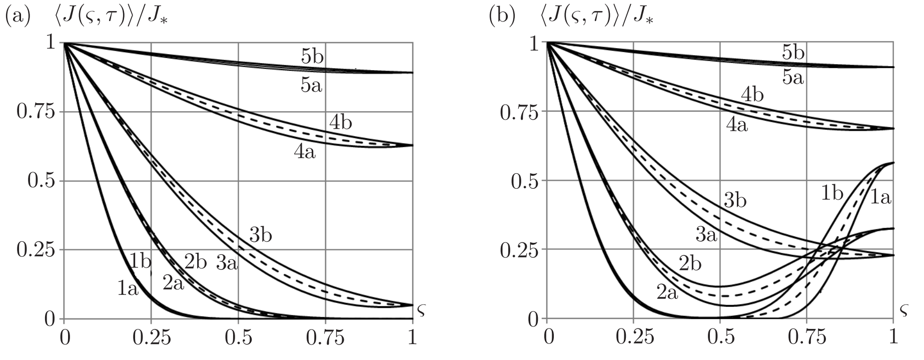

Figure 3. Distributions of mass flows in the strip in different moments of time at zero (a) and nonzero (b) initial concentrations

Figure 5 illustrates the behavior of averaged mass flows for different values of the volume fraction of inclusions $v_1 = 0.05$; 0.1; 0.2 (curves 1–3). Here curves a are built for $D_1/D_0 = 0.01$, curves b for $D_1/D_0 = 10$. Figure 6 shows the distributions of the flow function depending on both the degree of freedom of the function $f_1(\varsigma)$ $\alpha = 1.5$; 2.5; 3.5 (curves 1–3 in (a)) and the ratio $c_*/J_* = 0.01$; 0.1; 0.2; 0.3; 0.4 (curves 1–5 in (b)) at the nonzero constant initial concentration of admixture. Figures 3a–5a correspond to the case of zero initial concentration of admixture in the body, Figures 3b–5b correspond to the case of nonzero constant initial concentration. In Figures 3 and 6 curves a are used for $D_1/D_0 = 0.01$, curves b for $D_1/D_0 = 2$. The dash lines mark the corresponding flows in the homogeneous layer with the matrix characteristics.

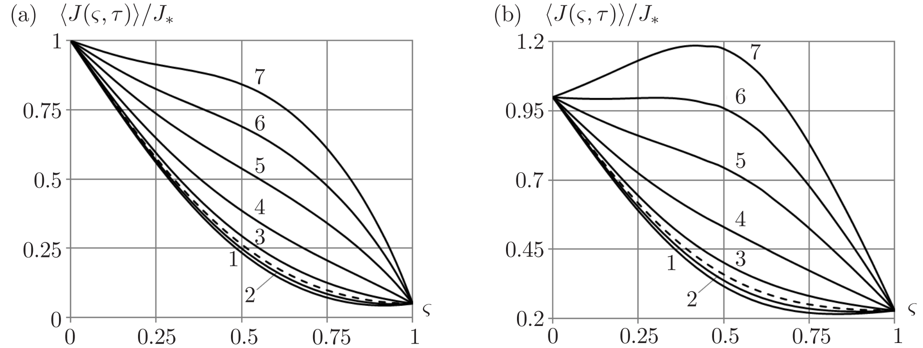

Figure 4. Distributions of mass flows in the strip depending on values of the ratio of diffusion coefficients D_1/D_0 at zero (a) and nonzero (b) initial concentrations

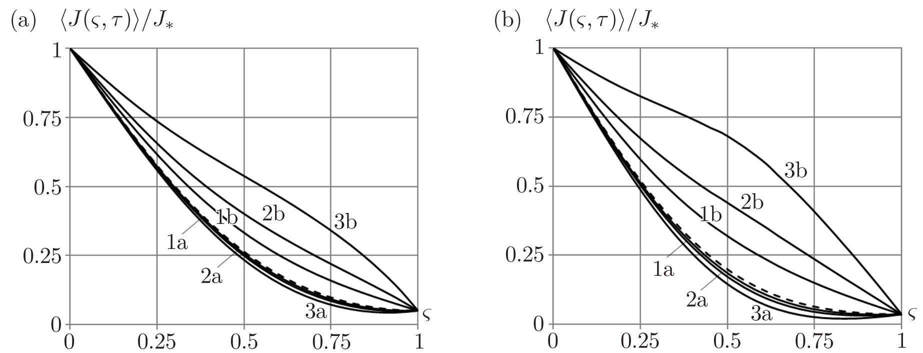

Figure 5. Distributions of mass flows in the strip for different values of the volume fraction of inclusions v_1 at zero (a) and nonzero (b) initial concentrations

Remark that as in the case of uniform distribution of inclusions in the body [17] admixture flows are steadily decreasing functions for $D_1 < D_0$ (Figure 3a). For $D_1 > D_0$ the function $\langle J(\varsigma,\tau)\rangle/J_*$ is also decreasing on all intervals for small differences of diffusion coefficients in inclusions and in the matrix, but an increase in the averaged flow from the surface where a mass source acts (curve 7 in Figure 4b) is observed for large difference between these coefficients.

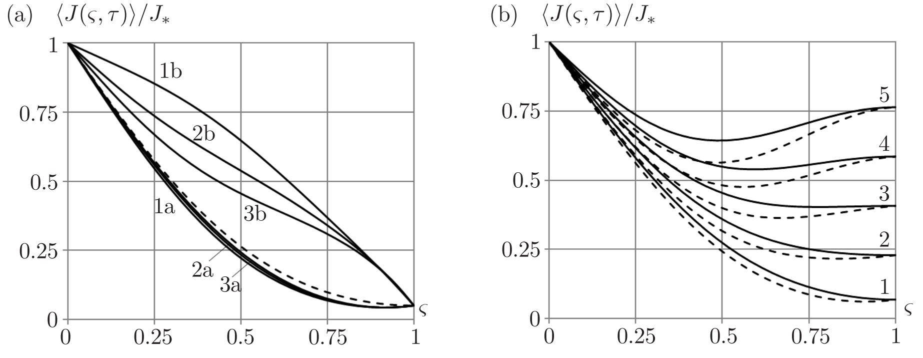

Figure 6. Distributions of mass flows in the strip for different values of the degree of freedom α (a) and the ratio c_*/J_* (b)

At a nonzero constant initial concentration of admixture the diffusion flow decreases from the boundary $\varsigma = 0$, it is close to zero in the middle of the layer and increases rapidly near the boundary $\varsigma = 1$ (curves 1a and 1b in Figure 3b). Moreover, the averaged mass flows from the body boundary, where the constant flow is supported, coincide sensibly with the flow in the homogeneous strip (curves 1 in Figure 3b) and begin to differ from each other from the middle of the layer and from the flow in the strip without interlayers. With the increasing time differences between the flows increase on the whole interval (curves 2 and 3 in Figure 3b), so, in particular, for $D_1/D_0 = 2$ the difference between the mass flows in the nonhomogeneous strip and homogeneous layer can reach 60%. Then, the difference between the flows decreases (curves 4 and 5 in Figure 3b) till they get a steady-state regime.

In the case where the coefficient of admixture diffusion in sublayers is greater than in the matrix, the flow in a nonhomogeneous body is always greater than in a homogeneous one (Figure 4). In the opposite case the flow in the multilayered strip is less than in the homogeneous layer (curves 1 and 2 in Figure 4). Herewith, an increase in the diffusion coefficient in inclusions in relation to the diffusion coefficient in the matrix leads to an increasing mass flow on all intervals (Figure 4), in particular, at a nonzero initial concentration the values of an averaged flow in the middle of the layer can be greater than its values on the "upper" boundary of the layer (curve 7 in Figure 4b). This situation is explained by a simultaneous increase in the flow through the "bottom" boundary of the body.

For the case of $D_1 < D_0$ an increase in the volume fraction of inclusions leads to decreasing mass flow values, and for $D_1 > D_0$ the increasing v_1 causes the flow to grow, especially on the interval $\varsigma \in [0.3; 0.8]$ (Figure 5). Remark that a change of the characteristic sublayer thickness almost does not affect the behavior of the averaged flow (a difference in the third significant digit).

If $D_1 < D_0$, then increasing the degree of freedom α (consolidation of inclusions to the lower surface) slightly affects the averaged flow values (curves a in Figure 6a). If the diffusion coefficient in inclusions is greater than in the matrix, then increasing the parameter α leads to a change of the flow function behavior. Hence, the flow function is convex upward at small values of α (curve 1b in Figure 6a), with the decreasing growth of α value of the averaged flow decreases and the function $\langle J(\varsigma,\tau)\rangle/J_*$ becomes concave in the interval $\varsigma \in [0; 0.6]$ (curve 3b in Figure 6a). Note that the behavior of the averaged diffusion flow is the same for different values of the degree of freedom α for both zero and nonzero initial concentrations in the body.

The values of the initial concentration affect both the behavior and values of the admixture flow function. For small values of the c_*/J_* ratio the admixture flow in both the homogeneous layer and the multilayered strip is steadily decreasing (curve 1 in Figure 6b). Increasing the initial concentration c_* leads to growth of the flow near the layer surface $\varsigma = 1$ that can lead to a local minimum in the middle of the layer (curves 4 and 5 in Figure 6b).

3.3. Diffusion flow in the strip with the most probable disposition of inclusions near the upper boundary

Consider another particular case of the β-distribution which will be obtained if we substitute $\alpha = 1$, $\beta \geq 1$ into the formula (16). The function of density of such distribution is as follows [21]

$$f_2(z) = \begin{cases} \beta\left(1 - \frac{z}{z_0}\right)^{\beta-1}, & z \in [0; z_0] \\ 0, & z \notin [0; z_0] \end{cases} \tag{30}$$

The case of distribution $f_2(z)$ is opposite to $f_1(z)$, namely on the upper surface of the body the inclusion sublayer is located with the probability 1, the region of the most probable disposition of inclusions is also lumped near this boundary, but on the lower body surface the matrix is situated a priori (Figures 7 and 8).

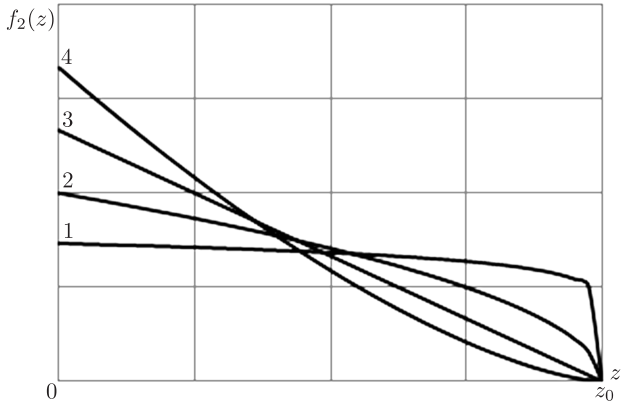

Figure 7. Density of distribution $f_2(z)$ for different degrees of freedom β

Plots of density of distribution $f_2(z)$ for different degrees of freedom $\beta = 1.1$; 1.5; 2; 2.5 (curves 1–4) are shown in Figure 7. In Figure 8 the corresponding

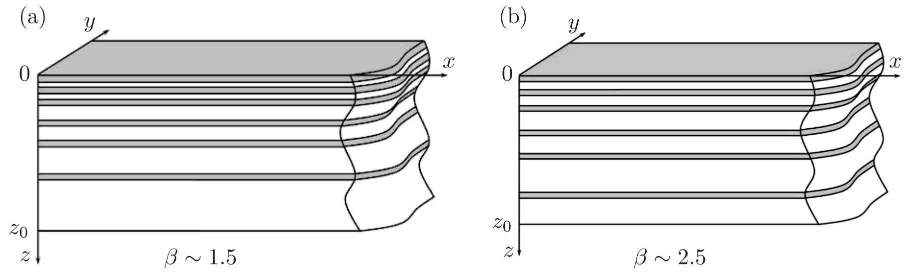

Figure 8. Possible structures of a multilayered strip with $f_2(z)$ distribution of inclusions

characteristic structures of multilayered strip are given. Note that in this case an increase in the value of the degree of freedom β leads to consolidation layered inclusions to the boundary $z=0$. At the same time the probability of inclusion location near another body boundary decreases.

As in the previous case, the random diffusion flow of admixture $J(z,t)$ in the structures of type shown in Figure 8 is described by the diffusion Equation (1). Assume that the conditions (2)–(4) are fulfilled and consider the case of zero and nonzero constant initial concentrations.

A solution of the initial-boundary value problem of diffusion in the two-phase multilayered strip with a region of the most probable disposition of inclusions near the upper body surface, where the mass source acts, is found in the form of the Neumann series (15). Restricted by two first terms of the series we perform the procedure of averaging it over the ensemble of phase configurations with the function of inclusion distribution $f_2(z)$ (30). As a result we obtain

$$\begin{aligned}\langle J(z,t)\rangle_{\mathrm{conf}} = J_0(z,t) + (D_1 - D_0)\int_0^t\int_0^{z_0} G(z,z',t,t')\frac{\partial J_0(z',t')}{\partial z'^2}\times \\ \times\sum_{i=1}^{n_1}\int_{(V)}\eta_{i1}(z')f_2(z_{i1})dz_{i1}dz'dt'\end{aligned} \tag{31}$$

In accordance with (21) we have

$$\sum_{i=1}^{n_1}\langle\eta_{i1}(z')\rangle = \sum_{i=1}^{n_1}\int_0^{z'}\eta_{i1}(x)f_2(z'-x)dx = \beta\sum_{i=1}^{n_1}\int_0^{z'}\eta_{i1}(x)\left(1-\frac{z'-x}{z_0}\right)^{\beta-1}dx \tag{32}$$

In particular, the following two cases are possible

(1) if $z' \le h_1$ then

$$\begin{aligned}\sum_{i=1}^{n_1}\int_0^{z'}\eta_{i1}(x)\left(1-\frac{z'-x}{z_0}\right)^{\beta-1}dx = \sum_{i=1}^{n_1}\int_0^{z'}\left(1-\frac{z'-x}{z_0}\right)^{\beta-1}dx = \\ = \frac{v_1}{\beta h_1 z_0^{\beta-2}}\left[z_0^{\beta} - (z_0 - z')^{\beta}\right]\end{aligned} \tag{33}$$

(2) if $z' \geq h_1$ then

$$\sum_{i=1}^{n_1}\int_0^{h_1}\eta_{i1}(x)\left(1-\frac{z'-x}{z_0}\right)^{\beta-1}dx=\frac{v_1}{\beta h_1 z_0^{\beta-2}}\left[(z_0-z'+h_1)^\beta-(z_0-z')^\beta\right] \quad (34)$$

Hence, for this inclusion distribution we obtain

$$\sum_{i=1}^{n_1}\langle\eta_{i1}(z')\rangle=\frac{v_1}{h_1 z_0^{\beta-2}}\begin{cases} z_0^\beta-(z_0-z')^\beta, & z'\leq h_1\\ (z_0+h_1-z')^\beta-(z_0-z')^\beta, & z'\geq h_1\end{cases} \quad (35)$$

Taking into account the expression (35) the averaged function (31) takes the form

$$\langle J(z,t)\rangle=J_0(z,t)+\frac{(D_1-D_0)v_1}{z_0^{\beta-2}h_1}\int_0^t\left[\int_0^{h_1}\left(z_0^\beta-(z_0-z')^\beta\right)G(z,z',t,t')\frac{\partial^2 J_0(z',t')}{\partial z'^2}dz'+\right.$$
$$\left.+\int_{h_1}^{z_0}\left((z_0+h_1-z')^\beta-(z_0-z')^\beta\right)G(z,z',t,t')\frac{\partial^2 J_0(z',t')}{\partial z'^2}dz'\right]dt' \quad (36)$$

Thus, we have obtained a formula for determining the diffusion flow averaged over the ensemble of phase configurations in a two-phase randomly nonhomogeneous multilayered strip with the most probable disposition of inclusions near the upper body boundary.

Substituting the expressions for the Green function (10) and the diffusion flow in a homogeneous strip at zero initial concentration (11) into the relation (36) we obtain the calculation formula

$$\frac{\langle J(z,t)\rangle}{J_*}=1-\frac{2}{z_0}\sum_{n=1}^{\infty}\frac{1}{\xi_n}e^{-D_0\xi_n^2 t}\sin(\xi_n z)+\frac{2(D_1-D_0)v_1}{D_0 z_0^\beta h_1}\times$$
$$\times\sum_{k=1}^{\infty}\sum_{n=1}^{\infty}\frac{\xi_n}{y_k^2-\xi_n^2}\left(e^{-D_0\xi_n^2 t}-e^{-D_0 y_k^2 t}\right)\left(a_{kn}z_0^\beta+A_{kn}^{(2)}\right)\sin(y_k z) \quad (37)$$

where $A_{kn}^{(2)}=\bar{f}(h_1,z_0+h_1,x_{kn}^-)-\bar{f}(h_1,z_0+h_1,x_{kn}^+)-\bar{f}(0,z_0,x_{kn}^-)+\bar{f}(0,z_0,x_{kn}^+)$, $\bar{f}(a,c,p)=\int_a^{z_0}(c-z)^\beta\cos(pz)dzsa$, $a_{kn}=\sin(x_{kn}^- h_1)/x_{kn}^- - \sin(x_{kn}^+ h_1)/x_{kn}^+$.

In the case of nonzero constant initial concentration in the body the calculation formula for the averaged diffusion flow is the following

$$\frac{\langle J(z,t)\rangle}{J_*}=1-\frac{2}{z_0}\sum_{n=1}^{\infty}e^{-D_0\xi_n^2 t}\left(\frac{1}{\xi_n}+(-1)^n\frac{D_0 c_*}{J_*}\right)\sin(\xi_n z)+$$
$$+\frac{2(D_1-D_0)}{D_0 z_0^\beta}\frac{v_1}{h_1}\sum_{k=1}^{\infty}\sum_{n=1}^{\infty}\frac{\xi_n}{y_k^2-\xi_n^2}\left(1+(-1)^n\frac{D_0 c_*}{J_*}\xi_n\right)\times \quad (38)$$
$$\times\left(e^{-D_0\xi_n^2 t}-e^{-D_0 y_k^2 t}\right)\sin(y_k z)\left(a_{kn}z_0^\beta+\bar{f}(h_1,z_0+h_1,y_k-\xi_n)-\right.$$
$$\left.-\bar{f}(h_1,z_0+h_1,y_k+\xi_n)-\bar{f}(0,z_0,y_k-\xi_n)+\bar{f}(0,z_0,y_k+\xi_n)\right)$$

We also calculate the integral summands in the expressions (37) and (38) by the method of trapezoids [23]. Perform numerical analysis of the obtained calculation formulae (36) and (37).

3.4. Simulation of averaged diffusion flows in the strip with the most probable disposition of inclusions near the "upper" boundary

On the basis of the formulae (37) and (38) modules of software have been designed for a qualitative and quantitative analysis of the averaged flow in a multilayered strip with a region of the most probable disposition of inclusions near the upper surface of the body, where the mass source acts.

Numerical calculations have been carried out in the dimensionless variables ς and τ (29). As numerical parameters of computation we have accepted $\tau = 0.1$; $v_1 = 0.2$; $h_1 = 0.01$; $\beta = 2.5$; $c_*/J_* = 0.1$. Figure 9 shows the distributions of mass flows in a different moment of dimensionless time $\tau = 0.01$; 0.03; 0.1; 0.5; 1 (curves 1–5) at zero (a) and nonzero constant (b) initial concentrations. Figure 10 illustrates the distributions of averaged diffusion flows for different values of the ratio $D_1/D_0 = 0.01$; 0.5; 2; 5; 10; 15; 20 (curves 1–7).

In Figure 11 the influence of the volume fraction of inclusions v_1 on the values of the averaged mass flow is shown, here curves 1–3 correspond to the values $v_1 = 0.05$; 0.1; 0.2. Figure 12 illustrates the dependence of the flow function on both the degree of freedom of distribution $f_2(\varsigma)$ $\beta = 1.5$; 2.5; 3.5 (curves 1–3 in Figure 12a) and the ratio $c_*/J_* = 0.01$; 0.1; 0.2; 0.3; 0.4 (curves 1–5 in Figure 12b).

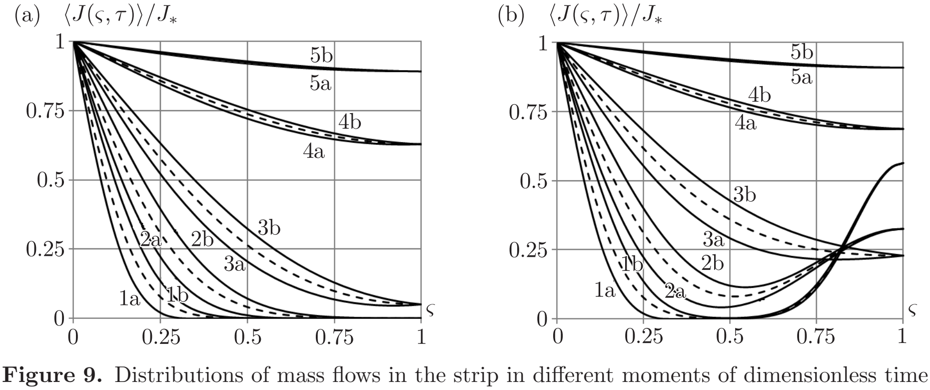

Figure 9. Distributions of mass flows in the strip in different moments of dimensionless time at zero (a) and nonzero (b) initial concentrations

Graphs in Figures 9a–11a are built for the case of zero initial concentration of admixture in the body; curves in Figures 9b–11b are calculated for nonzero constant initial concentration. In Figure 9 curves a are presented for $D_1/D_0 = 0.01$ and curves b for $D_1/D_0 = 2$. In Figures 11 and 12 curves a are presented for $D_1/D_0 = 0.01$ and $D_1/D_0 = 10$, respectively. Dash lines mark the flows in a homogeneous layer with the matrix characteristics.

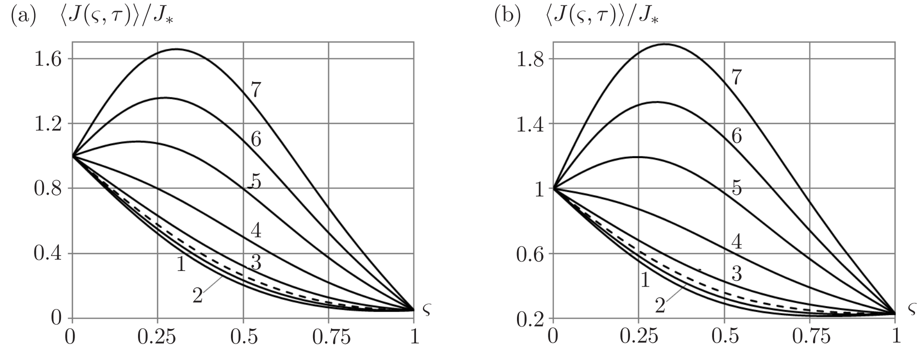

Figure 10. Distributions of mass flows in the strip for different values of the ratio D_1/D_0 at zero (a) and nonzero (b) initial concentrations

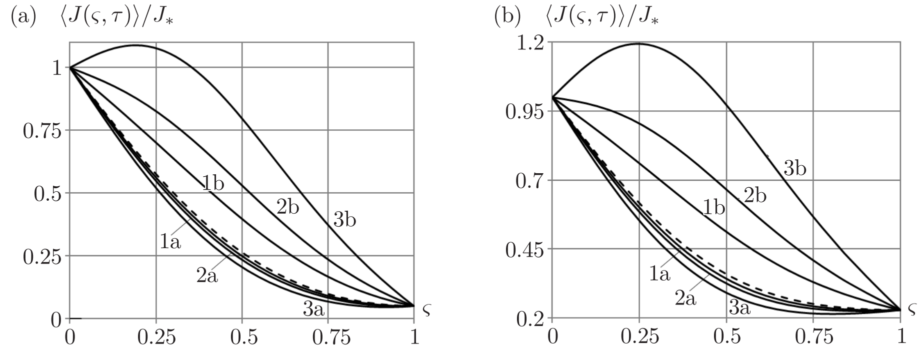

Figure 11. Distributions of mass flows in the strip for different values of the volume fraction of inclusions v_1 at zero (a) and nonzero (b) initial concentrations

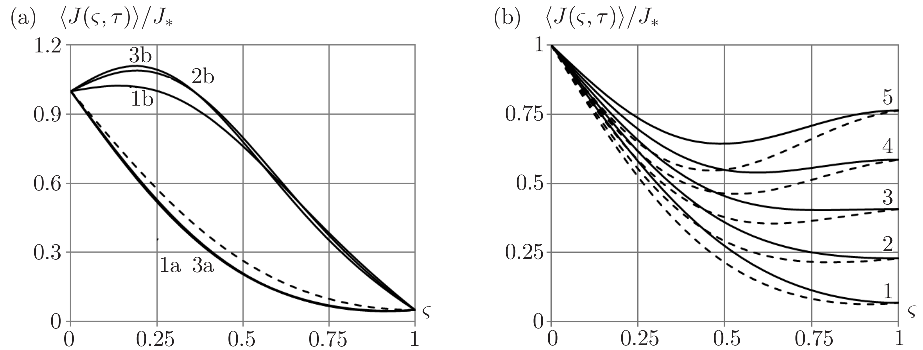

Figure 12. Distributions of mass flows in the strip for different values of the degree of freedom β (a) and the ratio c_*/J_* (b)

Note that for both $D_1 < D_0$ and $D_1 > D_0$ in the case of small values of derivation between diffusion coefficients in the matrix and inclusions the averaged admixture flows for zero initial concentration are steadily decreasing functions (curves 1–4 in Figure 10a). Here the values of the flows grow with time unless they get on the steady-state regime (Figure 9a). Where the inclusions are concentrated near the mass source there is a derivation up to 20% between the averaged flows in the nonhomogeneous strip and the homogeneous layer (curves 1a–3a and 1b–3b in Figure 9a) as opposite to the case presented in Figure 3a, where an appreciable difference is observed for moments of time $\tau > 0.5$ (curves 3a, 4a and 3b, 4b in Figure 3a).

The occurrence of a diffusing substance in the initial moment affects substantially the distributions of mass flows for small times of the running process of diffusion. Thus, for $\tau = 0.01$ the diffusion flow drops from the boundary $\varsigma = 0$, it is close to zero in the middle of the layer and grows rapidly near the boundary $\varsigma = 1$ (curves 1a and 1b in Figure 9b). With that the flows in homogeneous and nonhomogeneous strips differ substantially near the "upper" boundary, and almost the same for $\varsigma > 0.45$ (curves 1 in Figure 9b). With the increasing time difference between flows is first increasing over all the interval (curves 2 and 3 in Figure 9b) and then decreasing (curves 4 and 5 in Figure 9b) until flows get on the steady-state regime.

Increasing the ratio of diffusion coefficients D_1/D_0 leads to growth of the averaged diffusion flow at both zero and nonzero constant initial concentrations (Figure 10). In this case it is possible to form a global maximum in the middle of the layer which is greater by 15% at the nonzero initial concentration than at the zero one (curves 5–7 in Figure 10).

Note that for $D_1/D_0 < 1$ increasing the volume fraction of inclusions causes a decreasing value of the mass flow, but for $D_1/D_0 > 1$ the flow grows at both zero and nonzero initial concentrations (Figure 11). Moreover, for large values v_1 the averaged flow in the middle of the layer can become greater than its value on the upper body boundary (curves 3b in Figure 11).

There is practically no effect of change of the inclusion thickness h_1 on the value of the averaged diffusion flow at both zero and nonzero initial concentrations.

If the diffusion coefficient in inclusions is less than in the matrix, then increasing the degree of freedom β (consolidation of inclusions to the upper body surface) affects slightly the averaged flow value (curves a in Figure 12a). In the case of $D_1 > D_0$ increasing the value of the parameter β causes increasing values of the diffusion flow near the upper boundary of the strip, but does not change its behavior (curves b in Figure 12a). Remark that the behavior of the averaged diffusion flow for different values of the degree of freedom β is the same for both zero and nonzero initial concentrations in the body. A change of the ratio c_*/J_* influences both the behavior and values of the admixture flow function. Increasing the initial concentration c_* leads to growth of the flow near the layer surface $\varsigma = 1$ that can cause formation of a local minimum in the middle of the layer (curves 4 and 5 in Figure 12b).

3.5. Diffusion flow in the strip with the most probable disposition of inclusions in the middle of the body

Another particular case of the β-distribution is the distribution with the following function of density [21]

$$f_3(z) = \begin{cases} \frac{\Gamma(2\alpha)}{\Gamma^2(\alpha)} \left(\frac{z}{z_0}\right)^{\alpha-1} \left(1-\frac{z}{z_0}\right)^{\alpha-1}, & z \in [0; z_0] \\ 0, & z \notin [0; z_0] \end{cases} \tag{39}$$

which we obtain from the formula (17) for the values of the degrees of freedom $\alpha = \beta > 1$ [21].

Remark that under $\alpha = \beta = 1$ the distribution (39) coincides with the uniform one.

The distribution $f_3(z)$ describes a random stratified structure where the region of the most probable disposition of inclusions is situated in the middle of the body (Figures 13 and 14), herewith the matrix stands with probability 1 on the layer boundaries $z = 0$ and $z = z_0$.

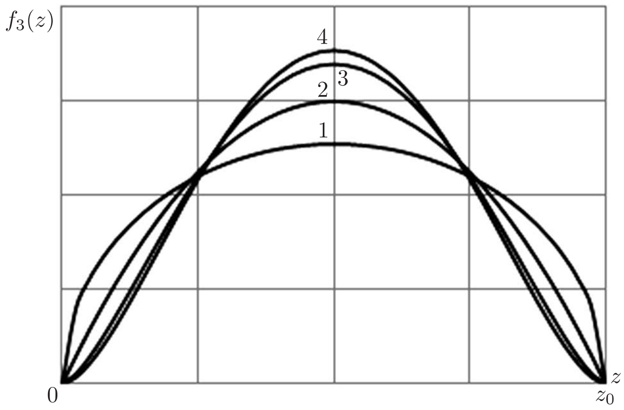

Figure 13. Density of distribution $f_3(z)$ for different degrees of freedom α

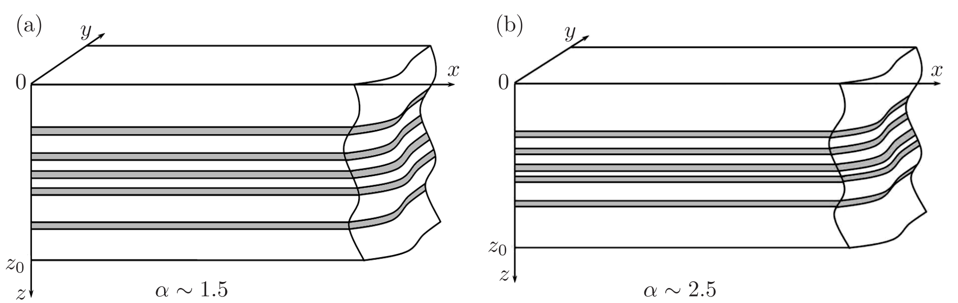

Figure 14. Possible structures of a multilayered strip with $f_3(z)$ distribution of inclusions

In Figure 13 peculiar densities of distribution $f_3(z)$ are illustrated for such values of the degree of freedom as $\alpha = \beta = 1.5$; 2; 2.5; 2.7 (curves 1–4). In Figure 14 characteristic structures of the multilayered strip are shown. Note that an increase in the parameter α leads to consolidation of inclusions to the middle of the body, and the region of the most probable disposition of inclusion is narrowed (Figure 14).

The flow of the admixture substance through the two-phase strip with an inner structure of the type shown in Figure 14, as in previous cases, is described by the diffusion Equation (1). Accept that the initial and boundary conditions on the flow function (2)–(4) are true. Here we shall also consider the cases of zero and nonzero constant initial concentrations of admixture particles.

We construct the solution of the initial-boundary value problem of diffusion (1)–(4) in the form of the Neumann series (15). Average the first two summands of the series over the ensemble of phase configurations with the function of inclusion distribution $f_3(z)$ (39):

$$\langle J(z,t)\rangle_{\mathrm{conf}} = J_0(z,t) + (D_1 - D_0)\int_0^t \int_0^{z_0} G(z,z',t,t')\frac{\partial J_0(z',t')}{\partial z'^2}\times \\ \times \sum_{i=1}^{n_1}\int_{(V)} \eta_{i1}(z')f_3(z_{i1})dz_{i1}dz'dt' \tag{40}$$

Similarly to (21) we have

$$\sum_{i=1}^{n_1}\langle \eta_{i1}(z')\rangle = \sum_{i=1}^{n_1}\int_0^{z'} \eta_{i1}(x)f_3(z'-x)dx = \\ = \frac{\Gamma(2\alpha)}{\Gamma^2(\alpha)}\sum_{i=1}^{n_1}\int_0^{z'} \eta_{i1}(x)\left[\left(\frac{z'-x}{z_0}\right)\left(1-\frac{z'-x}{z_0}\right)\right]^{\alpha-1}dx \tag{41}$$

Consider two following cases

(1) if $z' \le h_1$ then

$$\sum_{i=1}^{n_1}\int_0^{z'} \eta_{i1}(x)\left[\left(\frac{z'-x}{z_0}\right)\left(1-\frac{z'-x}{z_0}\right)\right]^{\alpha-1}dx = n_1\int_0^{z'}\left[z_0(z'-x)-(z'-x)^2\right]^{\alpha-1}dx \tag{42}$$

(2) if $z' \ge h_1$ then

$$\sum_{i=1}^{n_1}\int_0^{h_1} \eta_{i1}(x)\left[\left(\frac{z'-x}{z_0}\right)\left(1-\frac{z'-x}{z_0}\right)\right]^{\alpha-1}dx = n_1\int_0^{h_1}\left[z_0(z'-x)-(z'-x)^2\right]^{\alpha-1}dx \tag{43}$$

By calculating the corresponding integrals [22] the averaged "function of structure" with distribution $f_3(z)$ takes the form

$$\sum_{i=1}^{n_1}\langle \eta_{i1}(z')\rangle = \frac{Bv_1}{h_1 z_0^{\alpha-2}}\begin{cases} z'^{\alpha}\,{}_2\bar{F}_1(z'/z_0), & z' \le h_1 \\ z'^{\alpha}\,{}_2\bar{F}_1(z'/z_0) - (z'-h_1)^{\alpha}\,{}_2\bar{F}_1\big((z'-h_1)/z_0\big), & z' \ge h_1 \end{cases} \tag{44}$$

where $B=\frac{\Gamma(2\alpha)}{\alpha\Gamma^2}(\alpha)$, ${}_2\bar{F}_1(z)={}_2F_1(\alpha,1-\alpha;1+\alpha;z)$, ${}_2F_1(a,b;c;z)=\sum\limits_{m=0}^{\infty}\frac{(a)_m(b)_m}{(c)_m}\frac{z^m}{m!}$ is a hypergeometric function [22], $(a)_m=a(a+1)\dots(a+m-1)$, $(a)_0=1$.

Substitute the expression (44) into the relation (40), then we obtain a formula for determining the averaged diffusion flow of admixture particles in the two-phase strip with inclusions lumped in the middle of the body. Namely

$$\langle J(z,t)\rangle = J_0(z,t)+\frac{(D_1-D_0)Bv_1}{z_0^{\alpha-2}h_1}\int\limits_0^t\left[\int\limits_0^{z_0} z'^{\alpha}{}_2\bar{F}_1\left(\frac{z'}{z_0}\right)G(z,z',t,t')\frac{\partial^2 J_0(z',t')}{\partial z'^2}dz' - \right.$$
$$\left. -\int\limits_{h_1}^{z_0}(z'-h_1)^{\alpha}{}_2\bar{F}\left(\frac{z'-h_1}{z_0}\right)G(z,z',t,t')\frac{\partial^2 J_0(z',t')}{\partial z'^2}dz'\right]dt' \tag{45}$$

If we substitute the expressions for the Green function $G(z,z',t,t')$ (10) and the diffusion flow in the homogeneous layer $J_0(z,t)$ (11) into (45), then we obtain the calculation formula for the diffusion flow averaged over the ensemble of phase configurations at the zero initial concentration of admixture in the body

$$\frac{\langle J(z,t)\rangle}{J_*}=1-\frac{2}{z_0}\sum_{n=1}^{\infty}\frac{1}{\xi_n}e^{-D_0\xi_n^2 t}\sin(\xi_n z)+\frac{2(D_1-D_0)v_1 B}{D_0 z_0^{\beta}h_1}\times$$
$$\times\sum_{k=1}^{\infty}\sum_{n=1}^{\infty}\frac{\xi_n}{y_k^2-\xi_n^2}\left(e^{-D_0\xi_n^2 t}-e^{-D_0 y_k^2 t}\right)\bar{A}_{kn}\sin(y_k z), \tag{46}$$

where $\bar{A}_{kn}=f(0,0,x_{kn}^-)-f(0,0,x_{kn}^+)-f(h_1,0,x_{kn}^-)+f(h_1,0,x_{kn}^+)+$
$+\sum_{m=1}^{\infty}\frac{\alpha(1-\alpha)\dots(m-\alpha)}{z_0^m m!(m+\alpha)}\left[f(0,m,x_{kn}^-)-f(0,m,x_{kn}^+)-f(h_1,m,x_{kn}^-)+f(h_1,m,x_{kn}^+)\right]$,
$f(a,b,p)=\int_a^{z_0}(z-a)^{\alpha+b}\cos(pz)dz$.

If a nonzero initial concentration of admixture is imposed, then we use the formula (13) for $J_0(z,t)$ and the calculation formula for the averaged diffusion flow is as follows

$$\frac{\langle J(z,t)\rangle}{J_*}=1-\frac{2}{z_0}\sum_{n=1}^{\infty}e^{-D_0\xi_n^2 t}\left(\frac{1}{\xi_n}+(-1)^n\frac{D_0 c_*}{J_*}\right)\sin(\xi_n z)+\frac{2(D_1-D_0)v_1 B}{D_0 z_0^{\alpha}h_1}\times$$
$$\times\sum_{k=1}^{\infty}\sum_{n=1}^{\infty}\frac{\xi_n}{y_k^2-\xi_n^2}\left(e^{-D_0\xi_n^2 t}-e^{-D_0 y_k^2 t}\right)\left(1+(-1)^n\frac{D_0 c_*}{J_*}\xi_n\right)\bar{A}_{kn}\sin(y_k z) \tag{47}$$

Note that we shall also compute the integral summands in (46) and (47) by the method of trapezoids [23].

3.6. Flows in the strip with the most probable disposition of inclusions in the middle of the body

Let us analyze the dependence of the averaged diffusion flow in the two-phase multilayered strip with inclusions disposed after the distribution $f_3(\varsigma)$ on the input parameters of the problem at both zero and nonzero constant initial concentrations. In this case we also carry out numerical calculations in the dimensionless variables (29) by the formulae (46) and (47). We set the following values of coefficients as basic parameters of numerical investigation: $\tau = 0.1$; $v_1 = 0.2$; $h_1 = 0.01$; $\alpha = 2.5$; $c_*/J_* = 0.1$. In Figure 15 the behavior of the averaged diffusion flow in different moments of dimensionless time $\tau = 0.01$; 0.03; 0.1; 0.5; 1 is shown (curves 1–5). Figure 16 presents distributions of the mass flows in the strip under different values of the ratio of diffusion coefficients $D_1/D_0 = 0.01$; 0.5; 2; 5; 10; 15 (curves 1–6). Figure 17 illustrates the dependence of the flow function on different values of the volume fraction of inclusions, curves 1–3 correspond to $v_1 = 0.05$; 0.1; 0.2. Figure 18 shows distributions of the function $\langle J(\varsigma,\tau)\rangle/J_*$ depending on the degree of freedom of the function $f_3(\varsigma)$ $\alpha = 1.5$; 2.5; 3.5 (curves 1–3). In Figures 15, 17 and 18 curves a are used for $D_1/D_0 = 0.01$, curves b for $D_1/D_0 = 10$. Figures 15a–18a correspond to the case of the zero initial admixture concentration in the body, Figures 15b–18b correspond to the nonzero constant initial concentration. The dash lines mark diffusion flows in the homogeneous layer.

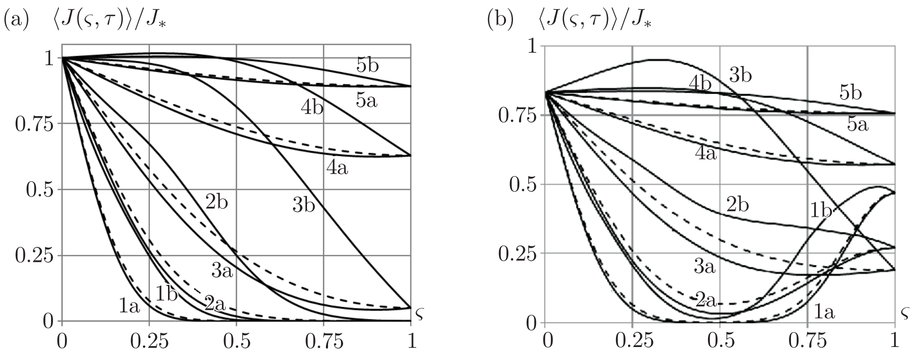

Figure 15. Distributions of mass flows in the strip in different moments of time at zero (a) and nonzero (b) initial concentrations

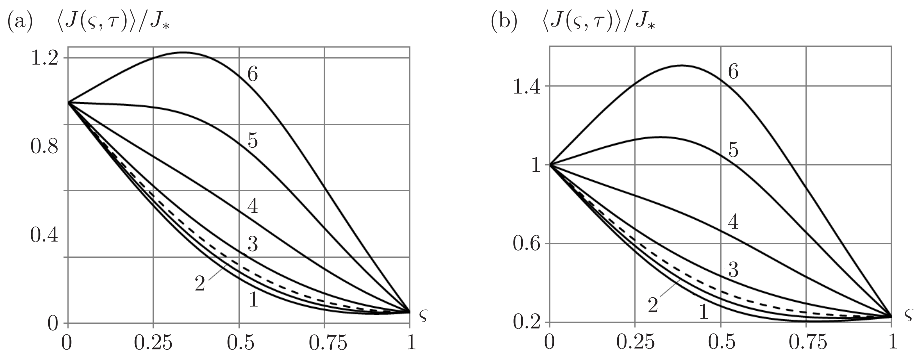

Figure 16. Distributions of mass flows in the strip for different values of the ratio D_1/D_0 at zero (a) and nonzero (b) initial concentrations

For the case of $D_1 < D_0$ the behavior of the averaged flow function is similar to the flow distributions in the stratified bodies with a subsurface region of the most probable disposition of inclusions. Note that at the zero initial

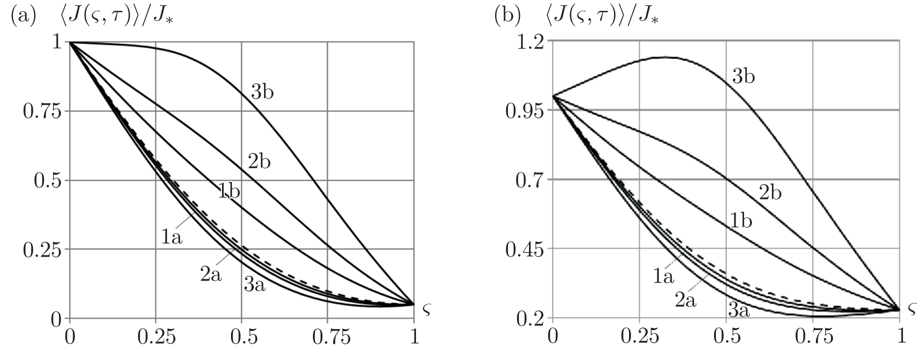

Figure 17. Distributions of mass flows in the strip for different values of the volume fraction of inclusions v_1 at zero (a) and nonzero (b) initial concentrations

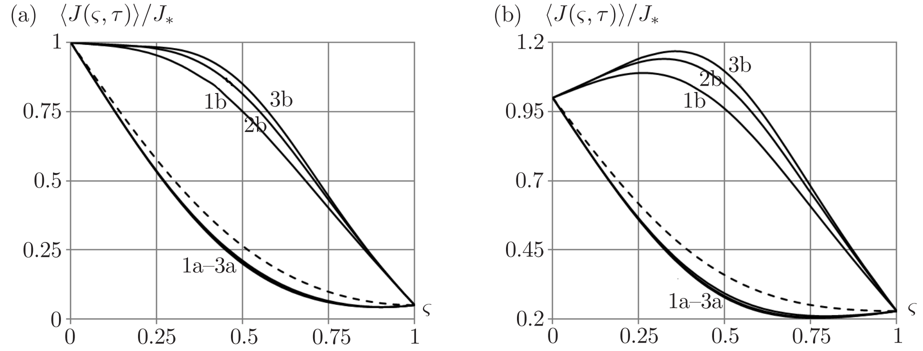

Figure 18. Distributions of mass flows in the strip for different values of the degree of freedom α at zero (a) and nonzero (b) initial concentrations

concentration if the diffusion coefficient is smaller than in the matrix, then the function $\langle J(\varsigma,\tau)\rangle/J_*$ is always steadily decreasing (curves a in Figure 15).

At the nonzero constant initial concentration for small times ($\tau < 0.02$) the diffusion flow drops from the boundary $\varsigma = 0$, it is close to zero in the middle of the layer and increases rapidly near the boundary $\varsigma = 1$ (curves 1 in Figure 15b). With the increasing time of the process of diffusion, in the case of $D_1 > D_0$, the averaged flow increases significantly, exceeding the values that are supported on the boundary $\varsigma = 0$ (curve 3b in Figure 15). Later the flow function remains convex upwards (curves 4b and 5b in Figure 15) and next its maximum decreases and vanishes while approaching the steady-state regime. Remark that unlike in previous cases, numerical calculations in this problem for curves b have been carried out for $D_1/D_0 = 10$. For the value $D_1/D_0 = 2$ we obtain the values of the averaged flow that are situated between the corresponding values for the structures with inclusion concentrations near one or another of the surfaces (Figures 3b and 9b).

By increasing the reduced diffusion coefficient the averaged mass flow increases on all intervals (Figure 16). The behavior of the function $\langle J(\varsigma,\tau)\rangle/J_*$ for zero and nonzero initial concentrations is similar (Figures 16a and 16b). Herewith for the nonzero initial concentration the averaged flow values are greater, differing by 24% at a maximum for $D_1/D_0 = 15$, $\varsigma = 0.38$ (curves 6 in Figures 16a and 16b).

An increase in the volume fraction of inclusions for $D_1/D_0 < 1$ causes decreasing values of the mass flow, but increasing the function $\langle J(\varsigma,\tau)\rangle/J_*$ for $D_1/D_0 > 1$ (Figure 17). In particular, at the nonzero initial concentration for large values of v_1 the averaged flow can be greater than its values on the upper body boundary (curves 3b in Figure 17b).

Consolidation of inclusions to the middle of the body for $D_1 < D_0$ influences neither the mass flow values nor the behavior (curves a in Figure 18). If the diffusion coefficient in inclusions is larger than in the matrix, then the consolidation of inclusions leads to an increase in the averaged flow at both zero and nonzero constant initial concentrations (curves b in Figure 18), mostly in the middle of the body.

Note that for the distribution $f_3(\varsigma)$ the dependence of the averaged diffusion flow on the value of the ratio c_*/J_* is similar to the cases of the inclusion distributions $f_1(\varsigma)$ and $f_2(\varsigma)$. For small values of the ratio c_*/J_* the admixture flow in both the homogeneous layer and the multilayered strip is a steadily decreasing function. With the increasing initial concentration c_* the flow grows near the body boundary $\varsigma = 1$, and it is possible to form a local minimum in the middle of the layer. As in previous cases, a change of the sublayer thickness h_1 does not practically affect the values of the averaged diffusion flow (difference in the third significant digit).

4. Comparison of the averaged flows for different model variants of inclusion disposition

Compare the behavior of the averaged diffusion flows in two-phase structures for the cases of uninform distribution of phases in the body [17] and particular variants of the β-distribution of sublayers (17), (30) and (39), where the region of the most probable disposition of inclusions occurs near one of the body surfaces (Figures 2 and 8) or in the middle of the strip (Figure 14).

Figures 19–23 illustrate comparative graphs of distributions of the averaged diffusion flows in the strip with uniform distribution of phases [17] (curves 1), the layers with regions of the most probable disposition of inclusions near the lower body surface (curves 2) and upper boundary (curves 3) calculated by the expressions (27), (28) and (37), (38), respectively as well as in the middle of the body (curves 4), calculated by the formulae (46) and (47). We set the following basic parameters of the problem: $\tau = 0.1$; $v_1 = 0.2$; $h_1 = 0.01$; $\alpha = 2.5$; $\beta = 2.5$ and $c_*/J_* = 0.1$. The dash lines mark the diffusion flows in the homogeneous body with the matrix characteristics. Figures 19 and 20 show the averaged diffusion flows at zero and nonzero initial concentration, respectively in different moments of dimensionless time $\tau = 0.01$ (a), $\tau = 0.03$ (b), $\tau = 0.1$ (c) and $\tau = 0.5$ (d) for $D_1/D_0 = 0.01$ (curves a) and $D_1/D_0 = 10$ (curves b). Figure 21 presents comparative distributions of the mass flows at zero (a) and nonzero constant (b)

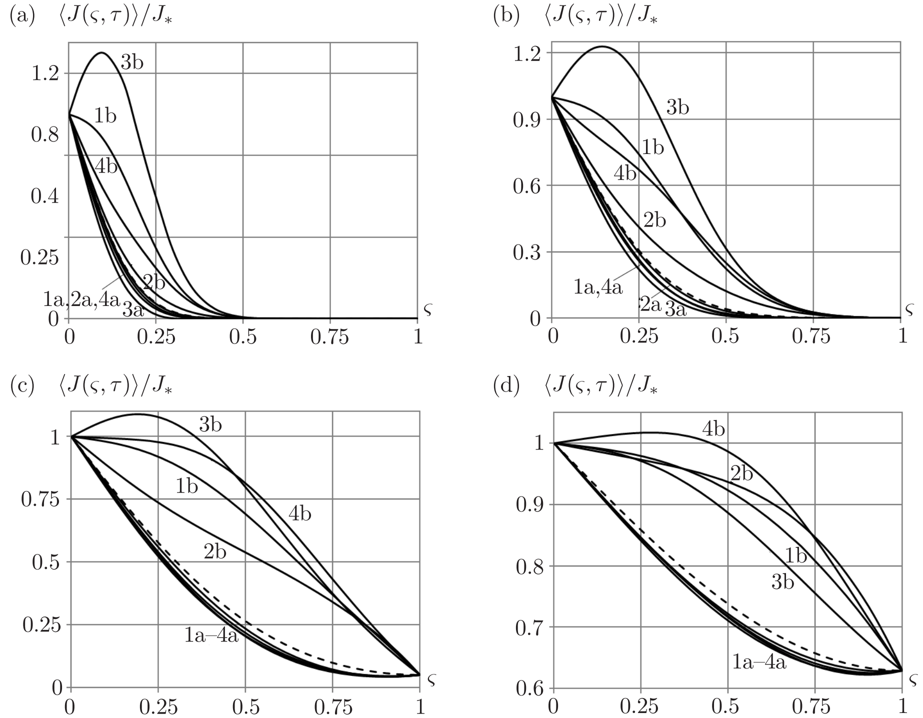

Figure 19. Distributions of mass flows at zero initial concentration for different model cases in moments $\tau = 0.01$ (a), $\tau = 0.03$ (b), $\tau = 0.1$ (c) and $\tau = 0.5$ (d)

initial concentrations for small and large volume fractions of inclusions v_1. Here curves a (dash-and-dot lines) describe the corresponding distributions for $v_1 = 0.05$, and curves b (full lines) for $v_1 = 0.1$.

Figure 22 shows comparative distributions of averaged diffusion flows at zero (a) and nonzero constant (b) initial concentrations depending on the ratio of diffusion coefficients in inclusions and in the matrix. Here curves a (dash-and-dot lines) are calculated for $D_1/D_0 = 5$, and curves b (full lines) for $D_1/D_0 = 15$.

Figure 23 illustrates comparative distributions of the admixture flows at the nonzero constant initial concentration depending on the ratio c_*/J_* values for $D_1/D_0 = 0.01$ (a) and $D_1/D_0 = 10$ (b). Here curves a (dash-and-dot lines) correspond to the distributions for $c_*/J_* = 0.01$, curves b (full lines) are calculated for $c_*/J_* = 0.4$ and curves 5 (dash lines) correspond to flows in the homogeneous body with matrix characteristics.

In the case of smaller values of the diffusion coefficient in the inclusion than in the matrix, for small times ($\tau < 0.1$) at the zero initial concentration the averaged diffusion flow in the structure with inclusions disposed near the upper body boundary is smaller up to 70% in the interval $\varsigma \in [0.1; 0.45]$ than the flows in the other three structures (curves 3a in Figures 19a and 19b). With the increasing time τ the difference between the flows drops (curves a in Figure 19c), and for $\tau = 0.5$ the averaged flows for different cases of dispositions of inclusions practically

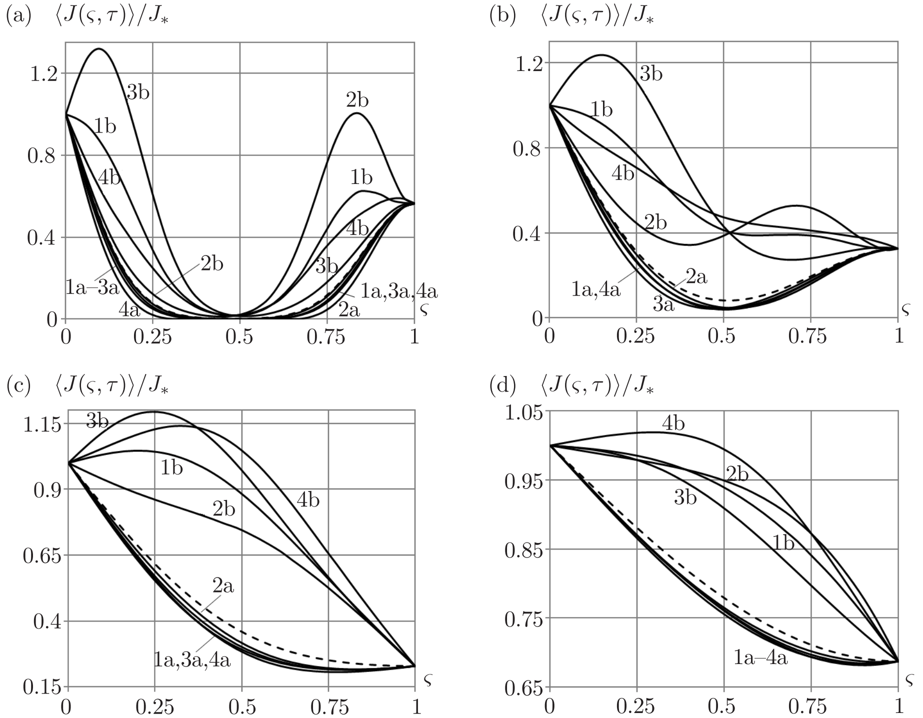

Figure 20. Distributions of mass flows at nonzero initial concentration for different model cases in moments $\tau = 0.01$ (a), $\tau = 0.03$ (b), $\tau = 0.1$ (c) and $\tau = 0.5$ (d)

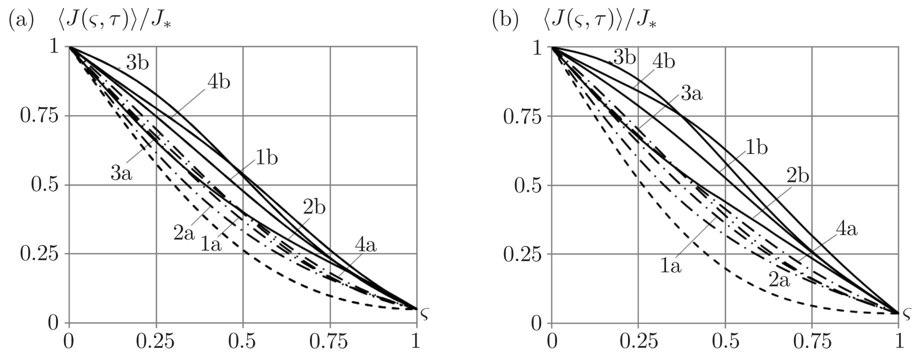

Figure 21. Distributions of mass flows at zero (a) and nonzero (b) initial concentrations for different model variants in dependence on the volume fraction of inclusions v_1

coincide (curves a in Figure 19d). If the coefficient of admixture diffusion in inclusions is larger than in the matrix, then for small times the diffusion flow in the strip with sublayers concentrated near the upper body boundary is the largest of the considered variants of the nonhomogeneity distributions and it forms the subsurface maximum (curves 3b in Figures 19a–19c), while for the other distributions of inclusions in the body the decreasing behavior of the averaged flows is characteristic (curves 1b, 2b and 4b in Figures 19a–19c). However, with

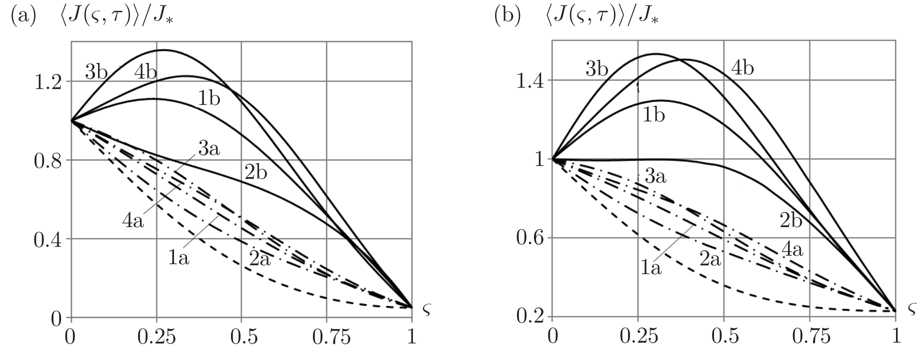

Figure 22. Distributions of mass flows at zero (a) and nonzero (b) initial concentrations for different model variants in dependence on the D_1/D_0 ratio

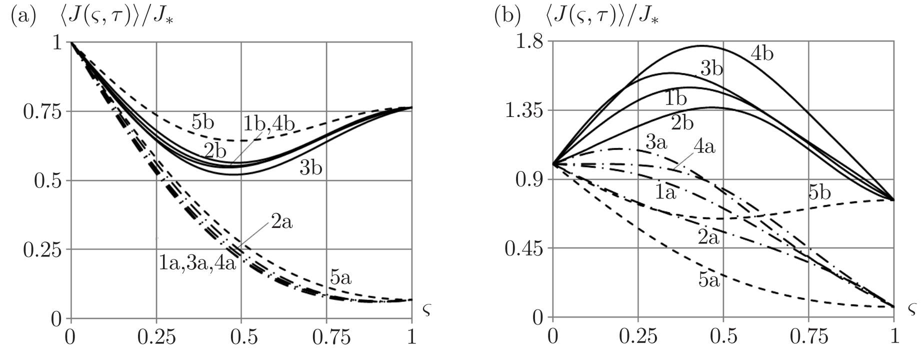

Figure 23. Distributions of mass flows at nonzero initial concentration for different model variants at $D_1/D_0 = 0.01$ (a) and $D_1/D_0 = 10$ (b) in dependence on the c_*/J_* ratio

increasing time the flow in the strip with a region of the most probable disposition of inclusions near the boundary $\varsigma = 0$ decreases and takes the smallest values of the three other flows (curve 3b in Figure 19d), and the averaged flow in the strip with sublayers located in the middle of the body becomes the greatest (curve 4b in Figure 19d). In the case of inclusion concentration near the lower body surface the function $\langle J(\varsigma,\tau)\rangle/J_*$ for $\tau < 0.1$ is convex downwards (curves 2b in Figures 19a and 19b), but for $\tau \geq 0.5$ it becomes convex upwards (curve 2b in Figure 19d). With a time increase the differences between flows in different model variants decrease until they reach a steady-state regime, where values of the flows coincide.

Note that at a nonzero constant initial concentration for $\tau < 0.03$ the admixture flows coincide from the boundary $\varsigma = 0$, except for flows in the structure where inclusions disposed near the upper surface of the body and the coefficient of admixture diffusion in inclusions is larger than in the matrix. Then, the diffusion flow increases sharply, and next it also becomes subsiding (curve 3b in Figure 20a). The admixture flows in all kinds of the structures begin to increase again from the middle of the strip (Figure 20a), but near the boundary $\varsigma = 1$ under $D_1/D_0 < 1$ the flow begins to decrease again for the body with the uniform distribution of inclusions, with probable dispositions near the lower boundary or in the middle of the strip (curves 1b, 2b and 4b in Figure 20a), i.e. the local maximum of the function $\langle J(\varsigma,\tau)\rangle/J_*$ occurs near the "bottom" body boundary. In the case of $D_1 < D_0$ for $\tau = 0.01$ the values of averaged flows coincide about in the structures with the uniform distribution of inclusions and their probable subsurface location in the interval $\varsigma \in [0;0.5]$ (curves 1a–3a in Figure 20a). The flow values in the strip with the most probable disposition of inclusions in the middle of the body are the smallest in this interval (curve 4a in Figure 20a). But in the interval $\varsigma \in [0.5;1]$ the flow in the strip with a probable disposition of inclusions near the lower body boundary takes the smallest values. Remark that in the case of $D_1 > D_0$ in the structures with the subsurface location of inclusions the presence of maximums of the diffusion flows near the surfaces where inclusions are concentrated is also observed (curves 2b and 3b in Figure 20a). With a time increase these maximums decrease and shift to the middle of the body (curves 2b and 3b in Figure 20b), and next the functions become steadily decreasing (curves 2b and 3b in Figure 20d). Moreover, for small times, the diffusion flow in the strip with the uniform distribution of phases is larger than in the strip with sublayers concentrated the middle of the body (curves 1b and 4b in Figure 20a), but for $\tau \geq 0.1$ the situation is reversed, namely the values of $\langle J(\varsigma,\tau)\rangle/J_*$ in the strip with the most probable distribution of inclusions in the middle of the body become larger than the flow values in the strip with uniform distribution of sublayers (curves 1b and 4b in Figure 20c). With increasing time τ of a process running distinction between the functions $\langle J(\varsigma,\tau)\rangle/J_*$ for different structures decreases and the flows reach a steady-state regime.

For the case where the diffusion coefficient in inclusions is greater than in the matrix, changes of the volume fraction of inclusions at zero and nonzero constant initial concentrations affect equally the behavior of the averaged flows for all kinds of the considered structures (Figure 21), slightly differing in the numerical results. In the case where the coefficient of admixture diffusion in inclusions is smaller than in the matrix, the averaged flows in stratified bodies are greater than the flow in the homogeneous body, and flow in the strip with sublayers concentrated near the lower boundary is the smallest of all cases considered (curves 2 in Figure 21). The growth of the value v_1 from 0.05 to 0.1 leads to an increase in the functions $\langle J(\varsigma,\tau)\rangle/J_*$ in all interval (curves b in Figure 21), and the difference between the flows in the strip with inclusions lumped near the upper and lower boundaries increases to 35% (curves 2b and 3b in Figure 21).

Note that for $D_1/D_0 \leq 5$ the averaged flows are decreasing functions (curves a in Figure 22). Growth of the ratio D_1/D_0 leads to increasing the flow, and its values can exceed the flow value on the "top" body boundary. Herewith the flow in the structure with probable distribution of inclusions near the surface where the mass source act, reaches the greatest values (curves 3b in Figure 22). For the considered values of input parameters of the problem, the maximums that the flows reach at zero initial concentration, are smaller to 19% than the maximums at nonzero a constant initial concentration of admixture (curves 1b, 3b and 4b in Figure 22).

If the coefficient of admixture diffusion in the matrix is larger than in inclusions, then an increase in the value of the initial admixture concentration reduced to the flow on the upper boundary of the strip c_*/J_* leads to the formation of a local minimum in the middle of the body for all the considered distributions of sublayers (curves b in Figure 23a). Moreover, the smaller the value c_*/J_*, the smaller the difference between the averaged diffusion flows for different kinds of stratified structures (Figure 23a). If the diffusion coefficient of the admixture substance in inclusions gets greater values than in the matrix, an increase in the c_*/J_* ratio causes an increase in the averaged admixture flow and formatting maximum of the functions $\langle J(\varsigma,\tau)\rangle/J_*$ in the middle of a two-phase strip for all the considered variants of inclusion dispositions (curves b in Figure 23b). In this case the greatest difference between the values of the flows, in particular, for structures with inclusions near the lower boundary and in the middle of the body can reach 30% (curves 2b and 4b in Figure 23b).

5. Conclusion

On the basis of the developed original approach we studied flows of the admixture substance in two-phase stochastically nonhomogeneous multilayered strips with non-uniform distributions of nonhomogeneities in the body domain. Within the scope of this approach the initial-boundary value problems were directly formulated for the functions of mass flow, the boundary conditions on one of the body surfaces were imposed for the function of mass flow and the conditions on admixture concentration were given on another boundary. Herewith the methods of constructing the solutions were adapted to the formulated problem. In particular, having considered the presence of stochastic nonhomogeneities as internal sources, the initial-boundary value problem with random coefficients was reduced to the equivalent integro-differential equation, the solution of which was constructed by the method of successive iterations in the form of absolutely and uniformly convergent Neumann series.

For the cases, where the region of the most probable disposition of inclusions crowds near the surface, where the mass source acts in the neighborhood of another body boundary and in the middle of the strip, we averaged the admixture flow over the ensemble of phase configurations at the zero initial condition for the function of diffusion flow that meant absence of admixture particles in the body in the initial moment or imposition of their nonzero constant initial distribution.

For different kinds of two-phase stratified structures we worked up the program modules for qualitative and quantitative analysis of dependence of the averaged diffusion flow on such medium characteristics as the ratio of diffusion coefficients, the volume fraction of inclusions, the specific (average) thickness of sublayers, etc. On this basis, simulation of the averaged diffusion flows of admixture in the multilayered strip was performed for different model variants of a probable disposition of phases in the body domain and their comparative analysis was made. In particular, it was shown that if the admixture diffusion coefficient in inclusions was smaller than in the matrix, then the location of inclusions in the body had almost no effect on the behavior of the averaged mass flows as on their values in most of the considered cases. Thus, we had to take into account the probable distribution of layered inclusions only as it was necessary to determine exact values of the mass flow function for small times. Instead, when the coefficient of admixture diffusion in inclusions took larger values than the diffusion coefficient in the matrix, the difference between the mass flows in different structures was significant and, for example, could reach 70% in the strip with inclusions concentrated near the upper boundary and in the strip with the most probable disposition of inclusions near the lower boundary. Herewith, for small times in the case of greater values of the diffusion coefficient of admixture in inclusions, the subsurface maximum was observed in the vicinity of the mass source for structures with inclusions located near the upper body boundary at both zero and nonzero constant initial concentrations. Nonetheless, the maximum of the averaged flow occurred near another body boundary for structures with uniform distribution of phases, with the inclusion concentrated in the middle of the body and near the lower boundary in the case of nonzero initial concentration. If inclusions were located after one of the partial case of beta-distribution, then for larger diffusion coefficient of admixture in inclusions there was a local that could be a global maximum of the flow in the middle of two-phase strip. At the same time, for the case of greater diffusion coefficient in the matrix, the global minimum of the averaged flow formed in the middle of the strip for large values of constant initial concentration for all the considered distributions of inclusions.

References

[1] Chaplya Y and Chernukha O 2009 *Mathematical modeling of diffusion processes in random and regular structures*, Naukova Dumka (in Ukrainian)

[2] Chaplya Y, Chernukha O, Goncharuk V and Torskyy A 2010 *Transfer processes of decaying substance in heterogeneous media*, Eurosvit (in Ukrainian)

[3] Chernukha O 2001 *Int. J. Heat and Mass Trans.* **44** 2535

[4] Chaplia Y and Chernukha O 2001 *J. Theor. and Appl. Mech.* **39** (4) 929

[5] Chaplia Y and Chernukha O 2003 *Int. J. Heat and Mass Trans.* **46** 3323

[6] Chaplya Y, Chernukha O and Bilushchak Y 2012 *J. Math. Sci.* **183** (1) 83

[7] Aslanov A M, Gerega A N and Lozovsky T L 2006 *J. Appl. Phys.* **76** (6) 134 (in Russian)

[8] Chen Z, Wu Y and Sun X 2015 *J. Wind Engineering and Industrial Aerodynamics* **137** 69

[9] Saeed A, Vuthaluru R and Vuthaluru B 2015 *Chemical Engineering Research and Design* **93** 79

[10] Gjennestad M A and Munkejord S T 2015 *Energy Procedia* **64** 53

[11] Bergins C, Crone S and Strauss K 2005 *Transport in Porous Media* **60** (3) 275

[12] Schulenberg T and Muller U 1987 *Int. J. Multiphase Flow* **13** (1) 87

[13] Lidzba D 1998 *J.Theor. and Appl. Mech.* **36** (3) 657

[14] Matysiak S J and Mieszkowski R 1999 *Int. Com. in Heat and Mass Trans.* **26** (4) 539

[15] Keller J 2001 *Transport in Porous Media* **43** (3) 395

[16] Chaplya Y Y, Chernukha O Y and Davydok A Y 2012 *Reports of the National Academy of Sciences of Ukraine* **11** 40 (in Ukrainian)

[17] Chaplya Y Y, Chernukha O Y and Davydok A Y 2015 *Task Quarterly* **19** (3) 297
[18] Crank J C 1975 *The Mathematics of Diffusion*, Clarendon Press
[19] Rytov S M, Kravtsov Y A and Tatarsky V I 1978 *Introduction to Statistical Radiophysic. Part II. Random fields*, Nauka (in Russian)
[20] Krasnov M L 1975 *Integral Equations*, *Nauka* (in Russian)
[21] Korolyuk V S, Portenko N I, Skorokhod A V and Turbin A F 1985 *Reference Work on a Probability Theory and Mathematical Statistics*, Nauka (in Russian)
[22] Abramowitz M and Stegun I 1964 *Handbook of Mathematical Functions with Formulas, Graphs and Mathematical Tables*, National Bureau of Standards (Applied Mathematics Series)
[23] Krylov V 1967 *An approximate calculation of integrals*, Nauka (in Russian)
[24] Lykov A V 1978 *Theory of Heat Conduction*, Higher School (in Russian)